



HAL
open science

Machine learning for temperature prediction in food pallet along a cold chain: Comparison between synthetic and experimental training dataset

Julie Loisel, Antoine Cornuéjols, Onrawee Laguerre, Margot Tardet,
Dominique Cagnon, Olivier Duchesne de Lamotte, Steven Duret

► To cite this version:

Julie Loisel, Antoine Cornuéjols, Onrawee Laguerre, Margot Tardet, Dominique Cagnon, et al.. Machine learning for temperature prediction in food pallet along a cold chain: Comparison between synthetic and experimental training dataset. *Journal of Food Engineering*, In press, 335, pp.111156. 10.1016/j.jfoodeng.2022.111156 . hal-03683454

HAL Id: hal-03683454

<https://hal.science/hal-03683454v1>

Submitted on 31 May 2022

HAL is a multi-disciplinary open access archive for the deposit and dissemination of scientific research documents, whether they are published or not. The documents may come from teaching and research institutions in France or abroad, or from public or private research centers.

L'archive ouverte pluridisciplinaire **HAL**, est destinée au dépôt et à la diffusion de documents scientifiques de niveau recherche, publiés ou non, émanant des établissements d'enseignement et de recherche français ou étrangers, des laboratoires publics ou privés.

Journal Pre-proof

Machine learning for temperature prediction in food pallet along a cold chain:
Comparison between synthetic and experimental training dataset

Julie Loisel, Antoine Cornuéjols, Onrawee Laguerre, Margot Tardet, Dominique Cagnon, Olivier Duchesne de Lamotte, Steven Duret



PII: S0260-8774(22)00210-2

DOI: <https://doi.org/10.1016/j.jfoodeng.2022.111156>

Reference: JFOE 111156

To appear in: *Journal of Food Engineering*

Received Date: 8 March 2022

Revised Date: 5 May 2022

Accepted Date: 26 May 2022

Please cite this article as: Loisel, J., Cornuéjols, A., Laguerre, O., Tardet, M., Cagnon, D., Duchesne de Lamotte, O., Duret, S., Machine learning for temperature prediction in food pallet along a cold chain: Comparison between synthetic and experimental training dataset, *Journal of Food Engineering* (2022), doi: <https://doi.org/10.1016/j.jfoodeng.2022.111156>.

This is a PDF file of an article that has undergone enhancements after acceptance, such as the addition of a cover page and metadata, and formatting for readability, but it is not yet the definitive version of record. This version will undergo additional copyediting, typesetting and review before it is published in its final form, but we are providing this version to give early visibility of the article. Please note that, during the production process, errors may be discovered which could affect the content, and all legal disclaimers that apply to the journal pertain.

© 2022 Published by Elsevier Ltd.

Julie Loisel: Conceptualization, Methodology, Software, Validation, Investigation, Data Curation, Writing - Original Draft, Visualization, Writing - Review & Editing

Antoine Cornuéjols: Conceptualization, Methodology, Resources, Data Curation, Writing-Reviewing and Editing, Funding acquisition

Onrawee Laguerre: Conceptualization, Methodology, Resources, Data Curation, Writing-Reviewing and Editing, Supervision, Funding acquisition

Margot Tardet: Conceptualization, Resources, Writing - Review & Editing, Supervision, Funding acquisition

Dominique Cagnon: Conceptualization, Resources, Supervision, Funding acquisition

Olivier Duchesne de Lamotte: Conceptualization, Resources, Supervision, Funding acquisition

Steven Duret: Conceptualization, Methodology, Investigation, Resources, Writing - Original Draft, Visualization, Reviewing and Editing, Supervision, Funding acquisition

1 **Machine learning for temperature prediction in food pallet**
2 **along a cold chain: comparison between synthetic and**
3 **experimental training dataset**

4 Julie Loisel^{1, 2, *}, Antoine Cornuéjols¹, Onrawee Laguerre², Margot Tardet³, Dominique
5 Cagnon³, Olivier Duchesne de Lamotte³, Steven Duret²

6 ¹ Université Paris-Saclay, UMR MIA-Paris, AgroParisTech, INRAE, 75005 Paris, France

7 ² Université Paris-Saclay, FRISE, INRAE, 92761 Antony, France

8 ³ BIOTRAQ, 6 Rue Montalivet, 75008 Paris, France

9 *Corresponding author Email address: julie.loisel@agroparistech.fr (Julie Loisel)

10 **Abstract**

11 Real-time prediction of product temperature is a challenge for cold chain monitoring. The use
12 of machine learning methods, especially neural networks, has been suggested as a possible
13 approach. However, their training requires a large amount of good quality data. We found that
14 experimental data leads to better results (by 20 to 40% compared with synthetic data) but require
15 material investment, while synthetic data generated from thermal model is plentiful but tends
16 to cause overfitting and overestimation of prediction performance (up to 150%). Our study
17 shows that increasing the amount of synthetic data only decreases the variance, but not the mean
18 error. The best strategy is to improve the thermal model used. As for experimental data, it is
19 more useful to find an optimal position of the sensor in the pallet than using ever increasing
20 realistic scenarios. Overall, even with imperfect predictions, machine learning models are able
21 to predict temperature in real time thus enabling to take preventive measures when needed.

22 **Keywords:** Temperature prediction, machine learning, synthetic data, experimental data, cold chain,
23 temperature abuse

24 **1. Introduction**

25 Food cold chain is composed of different stages: production (or harvest), product handling,
26 processing, distribution, and consumption. Temperature control along the cold chain is essential
27 to provide consumers with safe food of high organoleptic quality. Worldwide, it has been
28 estimated that 40% of food products require refrigeration (James and James 2010), and in
29 developed countries, 12% of losses of perishable foods is due to a lack of refrigeration (IIR
30 2021). A review of Ndraha et al. (2018) identified cold chain breaks in numerous studies. For
31 example, a field study in France showed that around 12% products in transport and distribution
32 had an average temperature above the recommended value (Derens et al. 2006). The recent
33 development of wireless temperature sensors at affordable prices enables real-time temperature
34 measurement along the cold chain (Bouzembrak et al. 2019).

35 Measuring and predicting the products' temperature in real-time are essential to detect cold
36 chain breaks and to estimate their impact on product quality. In practice, temperature sensors
37 such as Radio Frequency IDentification (RFID) tags are placed in the food stack to measure the
38 air temperature. One of the limitation in the use of such wireless sensors is that the temperature
39 is measured at one (or only at a few) position(s) in a pallet while products temperature is
40 heterogeneous (Laguerre et al. 2013). Hence, the measured temperature is not representative of
41 the full load. The temperature heterogeneity presents an issue when it comes about cold chain
42 break detection (Loisel et al. 2021). For example, a detection system may alert operators about
43 a cold chain break while products are not affected. Inversely, it may not detect and not alert the
44 operators while a corrective action would be necessary. Thus, the development of a model for

45 products' temperature prediction from measurement by few sensors located in a pallet is
46 appealing since it makes possible the detection of cold chain breaks.

47 In order to predict in real-time load temperature in refrigerating equipment from one or few
48 sensors, Badia-Melis et al. (2016) used thermodynamics based approaches such as kriging or
49 capacitive heat transfer models as well as machine learning methods. The authors showed that
50 predictions by physical based models were less precise in transitional state heat transfer than
51 in stationary state, which is an issue when detecting cold chain breaks. Overall, machine
52 learning models such as neural networks were more precise than physical based models and
53 have proved their performance in several other studies (Nunes et al. 2014; Hoang et al. 2021;
54 Mellouli et al. 2019; Mercier and Uysal 2018; Xiao et al. 2016).

55 Temperature data are necessary to train machine learning models for temperature prediction.
56 As discussed in Loisel et al. (2021), different sources of data are available: experimental data
57 (collected on field and in laboratory) and synthetic data (generated from simulation using
58 thermal models). However, field data are often incomplete (e.g., unknown environmental
59 conditions, few measured products), thus the options for different machine learning tasks are
60 limited. As alternatives, experimental data generated in laboratory and synthetic data generated
61 by thermal model are more robust to build a training dataset for machine learning models.
62 Indeed, all the temperatures at various locations on a pallet can be measured and calculated.
63 These two types of data involve different costs, different uncertainties, and different times.
64 Experimental data generation requires a controlled temperature test room, an experimental
65 device, a product to be tested and time to conduct the experiment (Duret et al. 2014). However,
66 this data can be assumed as representative of field data if physical properties such as ambient
67 air temperature or velocity are reproduced in the experimental room. Synthetic data generation
68 is less time consuming but it requires the use of thermal models, which can be obtained from
69 literature and from a specific development (Ambaw et al. 2021). As with all thermal models,

70 the uncertainty of temperature prediction is a common issue. The data uncertainty, related to
71 the applied assumptions, may affect the performance of a machine learning model trained with
72 those data.

73 The machine learning models used to predict product temperature in the cold chain reported by
74 several studies are based on both experimental (Badia-Melis et al. 2016) and synthetic data
75 (Mercier and Uysal 2018). However, to our knowledge, the precision of prediction by machine
76 learning models trained by these types of data were not compared in these studies.

77 This study aims to compare the use of experimental and of synthetic training data for machine
78 learning approaches using neural network (NN) models to predict product temperature
79 distribution in a pallet. The following questions are addressed:

- 80 • What is the impact of the sensor position on temperature prediction accuracy?
- 81 • Between experimental and synthetic data, which one allows obtaining the best
82 performance using machine learning models?
- 83 • Which strategies can be implemented to optimize the performances of the machine
84 learning models when only synthetic data is available?

85

86 **2. Material and methods**

87 **2.1. Overview of the methodology**

88 Figure 1 presents the overview of the methodology developed in this study. First, the data
89 sources are presented: namely an experimental set-up description (section 2.2.1) and the heat
90 balance equations for the developed thermal model (section 2.2.2). The data generated by
91 experiment and by thermal model according to different cold chain scenarios are presented
92 (sections 2.3.1 and 2.3.2). Then, the machine learning models trained on these two data sources

93 are described (section 2.4). Finally, their performances evaluated by using Root Mean Square
94 Error (RMSE) as criteria (section 2.5) are reported and compared (section 3).

95

96 **2.2. Data sources**

97 **2.2.1 Experimentation**

98 An experimental set-up (Figure 2) representing a level of a pallet (1.2m long, 1m wide and 0.1m
99 high) was installed inside a controlled-temperature test room of 29 m³ (3.4m long, 3.4m wide
100 and 2.5m high). Eight crates were filled with 28 apples each (*sp. Rubinette Rosso*, mass of an
101 apple = 120 g, diameter = 0.064 m). Two polystyrene plates (5 cm thickness) were placed at
102 the top and the bottom of the device to represent an intermediate level in a pallet. Air was sucked
103 through the device by 3 fans located at the exit enabling stable one-directional airflow. Air
104 velocity was fixed at 0.2 m.s⁻¹ at the entrance of the pallet to represent the pallet located in clam
105 air. Air flowed only through the space over the crates since the sidewalls were closed. The inlet
106 air temperature could be changed instantaneously by switching a shutter at different moments
107 to alternate between the cold air (of the test room) and warm air (previously flowing through a
108 heat resistance). Hence, different inlet air temperature profiles could be generated.

109 Temperatures were measured with T-type thermocouples previously calibrated at 0°C, 10°C,
110 20°C, 30°C and 40°C (precision +/-0.2°C). These thermocouples were placed at the core and
111 the neighboring air of 16 apples (2 apples/crate, Figure 2b). In addition, a thermocouple was
112 placed at the entrance of the device to measure the inlet air temperature. In each experiment,
113 the product initial temperature was considered as homogeneous while it was different in 10
114 studied scenario (see section 2.3). Temperatures were recorded every 20s for 12h.

115

116 2.2.2 Thermal model

117 A thermal model was developed to predict air and product temperatures at different positions
118 in a pallet using the inlet air temperature profile as input parameter. These predicted
119 temperatures are called synthetic data.

120 The model was based on a zonal approach. The model considers that a crate is composed of 2
121 zones, one near the side and one near the center of a pallet. Each zone is characterized by one
122 air and one core temperatures. Thus, a pallet level is composed of 16 zones.

123 As air flows through a pallet, it exchanges heat first with products upstream of the pallet.
124 Consequently, upstream products are more susceptible to variations in temperature as a result
125 of changes in ambient temperature. For this reason, temperature heterogeneity can be observed
126 in a pallet of product (Duret et al. 2014). The Biot number ($Bi = hR/\lambda$, ratio between internal
127 and external heat transfer resistances) of product is about 0.4 (where $R= 0.032$ m, $\lambda=0.39$ W.m⁻¹.K⁻¹
128 and $h=5$ W.m⁻².C⁻¹). Thus, the internal heat transfer resistance due to conduction inside
129 the apple is on the same order of magnitude as the convection and cannot be ignored.

130 In order to generate synthetic data, the numerical model used in this study used a zonal approach
131 to describe the evolution of air temperature through a pallet coupled with a 1D thermal model
132 to predict the product core temperature in each zone.

133 Assuming that in a zone, product temperature was homogeneous. Moreover, the heat transfer
134 by radiation was considered as negligible in this study.

135

136 *Air temperature calculation*

137 Only convective heat exchange between air and product was considered. At the time t , the inlet air
138 of temperature $T_{inlet,t}^{air}$ exchanges with product in the zone 1 (with convective heat transfer

139 coefficient h), this gives the air outlet of $T_{1,1,t}^{air}$, which is the inlet air of the zone 5 and so on. The
 140 generalization of the balance equation over 16 zones is presented as follows:

$$141 \quad \dot{m} \times C_p^{air} \times (T_{i,j,t}^{air} - T_{i-1,j,t}^{air}) + h \times S \times (T_{i,j,t}^{air} - T_{i,j,t}^{prod,s}) = 0 \quad (1)$$

142 With \dot{m} , the air mass flow rate ($\text{kg}\cdot\text{s}^{-1}$), C_p^{air} the air heat capacity ($\text{J}\cdot\text{kg}^{-1}\cdot\text{°C}^{-1}$), $T_{i,j,t}^{prod,s}$ the
 143 product surface temperature (°C), S the product surface area (m^2) and h the convective heat
 144 transfer coefficient between air and product surface was considered as constant in all 16 zones.
 145 Both free and forced convection can be considered for low air velocity used in our study (0.2
 146 $\text{m}\cdot\text{s}^{-1}$). The corresponding convective heat coefficient $h = 5 \text{ W}\cdot\text{m}^{-2}\cdot\text{C}^{-1}$ was obtained by fitting
 147 product core temperature change with time during a cooling from 20°C to 4°C (independent
 148 scenario from all scenarios presented next in this work). This value in the condition of our study
 149 corresponds to mixed convection (Richardson number $= Gr/Re^2 \sim 0.8$) and is in agreement with
 150 previous values observed in pallets in the literature (min= $2 \text{ W}\cdot\text{m}^{-2}\cdot\text{C}^{-1}$ and max= $20 \text{ W}\cdot\text{m}^{-2}\cdot\text{C}^{-1}$;
 151 Duret et al. 2014, Laguerre et al. 2014).

152 ***Product temperature calculation***

153 For simplification, an apple was considered as a sphere with no heat generation and constant
 154 thermal diffusivity α ($\alpha = 1.1 \times 10^{-7} \text{ m}^2\cdot\text{s}^{-1}$). Inside a product, conduction only in radial
 155 direction was considered (1D model). The transient heat conduction equation in spherical
 156 coordinates is:

$$157 \quad \frac{1}{\alpha} \frac{\partial T}{\partial t} = \frac{1}{r^2} \frac{\partial}{\partial r} \left(r^2 \frac{\partial T}{\partial r} \right) \quad (2)$$

158 Symmetry and convective boundary conditions were considered in product core and surface,
 159 respectively:

$$160 \quad \left. \frac{\partial T}{\partial r} \right|_{r=0} = 0 \quad (3)$$

161
$$-\lambda \left. \frac{\partial T}{\partial r} \right|_{r=R} = h(T^{air} - T^{prod,S}) \quad (4)$$

162 At $t = 0$, $T_{i,j,t}^{prod} = T_0$ (homogeneous product initial temperature in all zones).

163 This equation was solved using FTCS (Forward Time Centered Space) method (Thibault et al.
164 1987). At the top and the bottom of the experimental device, adiabatic walls are considered to
165 represent an intermediate layer in a pallet.

166 **2.3. Data generation from different cold chain scenarios**

167 **2.3.1. Experimental dataset**

168 Ten profiles of the inlet air temperature (T_{inlet}^{air}) were created using the experimental device to
169 represent 10 cold chain scenarios for a fixed duration of 12h each (Figure 3 A & B). These
170 scenarios were built by combining cooling and warming events at the inlet air temperature to
171 represent the ones observed in real situations, e.g. products loading/unloading in a cold
172 equipment, temperature fluctuations due to on/off cycles of compressor, defrosting during
173 which compressor is turned off, product transferred from one to another cold equipment in
174 which the set temperatures are different...). The mean and standard deviation of the inlet air
175 temperature in these scenarios were different in order to represent as much as possible real
176 conditions. It is to be emphasized that for one scenario, a core and an air temperature in 16
177 zones in the experimental set-up were generated.

178 **2.3.2. Synthetic dataset**

179 The air inlet temperature profiles, used as inputs of thermal model for synthetic data generation
180 (Figure 3 C & D), were obtained by applying a moving average smoothing method on the
181 experimental profiles. In this manner, noiseless data was generated from the same 10 scenarios.

182 Similarly to the experimental dataset, each scenario generated a core and an air temperatures in
 183 the 16 zones.

184 **2.4 Machine learning models**

185 Numerous machine learning models exist in the literature. Only the results obtained with neural
 186 networks are reported in this work. Neural networks are representative of machine learning
 187 methods with the same issue of generalizing from data while avoiding overfitting. In addition,
 188 we obtained better results with neural networks than with ensemble methods such as Random
 189 Forests and Adaboost, as well as linear methods such as Linear Regression, Lasso, and SVM.
 190 Therefore, results obtained with neural networks are indicative of what one can hope for using
 191 the best machine learning method to date on that type of learning task.

192 The conclusions we reached in our experimental study would remain qualitatively the same if
 193 we had used other machine learning methods, but with inferior performance. Since we are
 194 comparing synthetic and experimental data, neural networks were selected to alter their
 195 architecture. This was done to see if the difference between the two training datasets was the
 196 same for different architectures.

197 **2.4.1 Inputs and output of the Neural Network (NN)**

198 The objective of a NN is to predict the products' core temperatures in each 16 zones from an
 199 air temperature measurement, as in field practice. Hence, the NNs were trained to predict the
 200 16 apples' core temperature at time t ($T_{i,j,t}^{core}$) knowing the air temperature inside the pallet at
 201 the previous time steps ($T_{i,j,t-\lambda\Delta t}^{air}, T_{i,j,t-(\lambda-1)\Delta t}^{air}, \dots, T_{i,j,t-\Delta t}^{air}$) (Figure 4). In each of the 16 zones,
 202 indices i and $j = [1,..4]$ represent the coordinates of the position of the zone in the experimental
 203 set-up (Figure 2.b), $\lambda\Delta t$ the time delay between the last measurement (at $t = t - \Delta T$) and the

204 oldest measurement (at $t = t - \lambda \Delta T$) used as input of the NN, Δt the time step between two
205 measurements. According to our preliminary study, $\lambda = 50$ is an optimal value.

206 **2.4.2 Tested NN architectures**

207 The type of NN used is the Multilayer Perceptron Regressor (MLP), that uses back propagation
208 and stochastic gradient descent to optimize the squared loss. The activation function for the
209 hidden layers was the Rectified Linear Unit function (RELU). For all tested NNs, the
210 hyperparameters (e.g. α : L2 penalty parameter) were set at the default values of the library
211 scikit-learn (Pedregosa et al. 2011). In this case, the multi-output version of the MLP was
212 implemented: the output layer's size is 16, corresponding to the 16 apple core temperatures.
213 The objective of this work is not to find the best model, but to compare the quality of the training
214 data. Tests were performed on various NN architectures, from 1 hidden layer to 3 hidden layers
215 to evaluate the impact of different strategies (noise addition, data augmentation). The different
216 sizes of the hidden layers were chosen according to preliminary simulations. Finally, 5 different
217 hidden layer architectures were presented in this work:

- 218 • 1-hidden layer architectures: 5 and 15
- 219 • 2-hidden layers: (10, 4)
- 220 • 3-hidden layers: (5, 5, 5) and (24, 12, 4)

221 **2.5 Performance evaluation**

222 The models were trained and tested through a *leave-one out* (LOO) cross-validation procedure.
223 This procedure evaluates the model's capacity to predict the target on an unknown profile. In
224 our case, a dataset includes 10 temperature scenarios (16 air temperatures and 16 core
225 temperatures in each). A model was trained on 9 scenarios (scenarios 2 to 10) then tested on
226 the remaining scenario (scenario 1- see Figure 5). This process was repeated 10 times. In the

227 second step, scenario 2 is used for the test, in third step, scenarios 3 is used for the test and so
 228 on. The LOO cross-validation procedure enables estimating the performance of the model when
 229 generalizing to an independent real scenario.

230 It is of major importance to emphasize here that the scenario used for the test are always
 231 experimental. Even when NNs are trained with synthetic data, the performance is evaluated by
 232 testing in comparison with experimental data. In this way, the NN models trained with the
 233 experimental and synthetic datasets are evaluated on the same data and their performance
 234 comparison is possible. Moreover, it corresponds to the field operational conditions as these
 235 NNs are meant to predict temperature from a wireless sensor placed in a pallet.

236 The chosen performance criteria was the Root Mean Square Error (RMSE) since it is
 237 appropriate for numerical predictions:

$$238 \quad RMSE = \sqrt{\frac{\Delta t}{N_{zone} \times t_{max}} \sum_{n=1}^{N_{zone}} \sum_{t=0}^{t_{max}} \frac{\Delta t}{\Delta t} (\hat{T}_{n,t}^{core} - T_{n,t}^{core})^2} \quad (3)$$

239 With the number of zones $N_{zone} = 16$, the time step $\Delta t = 60s$, $t_{max} = 12 \times 3600s$. $T_{n,t}^{core}$
 240 and $\hat{T}_{n,t}^{core}$ are respectively the measured and predicted (by the NN) core temperatures of the
 241 apple of the zone n at time t .

242 Furthermore, NN training uses pseudo-random numbers generated from a random seed. The
 243 same model trained on the same data with different random seeds will not give us the same
 244 results. The random seed has an impact on how the NN weights are initialized.

245 Depending on the analysis provided, some specifications of the RMSE calculation are given:

246 **2.5.1. Performance over the 10 scenarios.** In sections 3.1, 3.2 and 3.3, the $RMSE_s$ is used.
 247 $RMSE_s$ is based on $RMSE$ defined in (3). In the LOO cross validation process (Figure 5.A), for
 248 each of the 10 training and testing steps s , a total of 50 iterations with different random seeds

249 are processed, resulting in 50 $RMSE_{s,i}$. Then, the average value is calculated ($RMSE_s$) and
 250 presented by boxplots describing the distribution of the 10 $RMSE_s$. In other words, these
 251 boxplots represent the performances distribution according to the 10 temperature scenarios.
 252 This allows us to present results that are independent from the random seed and hence
 253 independent from the NN initialization.

254 **2.5.2. Performance over time.** In Figure 7 (section 3.2), the evolution of the NN performance
 255 over time is studied, this is represented by a $RMSE_t$:

$$256 \quad RMSE_t = \sqrt{\frac{\Delta t}{N_{zone} \times t_{max}} \sum_{n=1}^{N_{zone}} \sum_{u=0}^t \frac{t}{\Delta t} (\hat{T}_{n,u}^{core} - T_{n,u}^{core})^2} \quad (4)$$

257 With t the time at which the $RMSE_t$ is calculated. For example, at time $t = 2h$, the $RMSE_t$ from
 258 time $u = 0h$ to $u = 2h$ is calculated.

259 **2.5.3. Average performance over 50 different weight initializations.** In section 3.4 (Impact
 260 of additional synthetic data), the $RMSE_i$ is used. $RMSE_i$ is also based on the $RMSE$ (see
 261 equation 3). The LOO cross validation (Figure 5.A) is processed for a given seed for the 10
 262 steps s , resulting in 10 $RMSE_{s,i}$ (Figure 5.B) which are averaged. This process is conducted 50
 263 times with 50 different random seeds (i.e., NN initializations, data shuffle ...) resulting in 50
 264 $RMSE_i$. The corresponding results are presented using boxplots describing the distribution of
 265 the 50 $RMSE_i$ of each iteration i (seed setting); in other words, the model performance
 266 according to 50 different NN initializations.

267

268 **3. Results & Discussion**

269 **3.1. Position of the temperature sensor in the pallet.**

270 All sensors' positions were tested, but only two results with sensors placed at the front and at
271 the back are presented. Figure 6 shows the $RMSE_s$ distribution according to the sensor's
272 position in the pallet and the architecture of the tested NN. Among the different proposed NNs
273 (number of hidden layers, hidden layer size), none of the architectures showed consistently
274 better performances. In single-sensor configurations, the NN performances are better when the
275 sensor is placed at the back ($RMSE_i = 0.95$; downstream airflow) than at the front of the pallet
276 ($RMSE_i = 1.41$; upstream airflow). Results agree with similar studies in the literature (Badia-
277 Melis et al. 2016; Mercier and Uysal 2018). Indeed, the air temperature (measured by the
278 sensor) in the back depends on the air and product temperatures located at the upstream
279 positions in the pallet. In other words, the evolution of the air temperature at the back contains
280 information about the air and product temperatures of the previous zones. The air temperature
281 at the front, on the other hand, depends mostly on the external ambient air. In field conditions,
282 it is difficult to control the airflow direction around a pallet. Moreover, the pallet position in an
283 equipment can change through the cold chain, e.g. a crate at the back (downstream airflow) in
284 a specific equipment can become the crate at the front (upstream airflow) in another equipment.
285 Taking into consideration this fact, when only one sensor is available, it should be placed at the
286 center of the pallet: either at the two opposite sides in a pallet (Mercier and Uysal 2018). These
287 two sensor positions would allow more robust results ($RMSE_i = 0.65$), but at a higher cost. A
288 cost analysis should take into consideration the performance of the cold chain break detection
289 system, its implementation cost (linked to the number sensors), product economical value and
290 cost of product losses following cold chain break. This analysis would help the decision-making
291 of the most appropriate solution for a given product.

292

293 **3.2. Evolution of model performance over time**

294 The core temperature evolutions (average value of 16 measurements) and the predicted ones
295 (by NN) are presented in Figure 7.A, and the comparison of $RMSE_t$ evolution for the NN
296 trained with experimental and synthetic data presented in Figure 7.B. It is obvious that the
297 core temperature is poorly predicted during the first hour ($RMSE_t > 2$), then, the
298 $RMSE_t$ decreases rapidly over time ($RMSE_t < 1$). This can be explained by the fact that at
299 time $t = 0$, the NN does not have the data of the initial product temperature. Indeed, in
300 practice, the sensor is placed in the pallet and measures the air temperature, no data of product
301 temperature provided to the NN. The precision of prediction increases with time, this can be
302 explained by the fact that the product measured and predicted temperatures (by NN) reach
303 progressively the inlet air temperature. In practice, in order to avoid false or undetected cold
304 chain breaks, the sensor should be placed in the pallet long time before shipping. In this
305 manner, the NN will be able to determine a product temperature in controlled conditions and
306 then to predict the product temperature correctly after shipping.

307

308 **3.3. Influence of data source on NN model performance**

309

310 **3.3.1 Comparison of model performances**

311 The performances of the NNs trained with two data sources (experimental and synthetic) are
312 shown in Figure 8 for two sensor positions (back and front). For all tested NNs, the $RMSE_s$ of
313 the NNs trained with experimental data are lower than the $RMSE_s$ of the NNs trained with
314 synthetic data. These results were expected as the calculation of the $RMSE_s$ for the data sources
315 are performed on experimental data. Moreover, this is also due to the uncertainty of the
316 synthetic data as this dataset was generated from a numerical model with its own uncertainty.
317 However, the difference of the performances between the two types of data is lower when the

318 sensor is located at the back of the pallet (up to 0.2 °C corresponding to 20%; Figure 7.A) than
319 when the sensor is placed at the front (up to 0.6 °C corresponding to 40%; Figure 7.B). Although
320 NNs trained with experimental data show better performances, their generation has constraints.

321

322 **3.3.2 Estimation of the model performance without experimental data**

323 Although it is possible to train NNs with synthetic data, the evaluation of an NN performances
324 without any experimental or field data is more complex. When no experimental data is
325 available, one would have to train NNs on synthetic data. In this case, the LOO cross-validation
326 process would be conducted using also synthetic data as test data. However, as observed in
327 Figure 9, the $RMSE_s$ estimated using synthetic noiseless data as test data ($0.7 \pm 0.35^\circ\text{C}$) are
328 lower than the $RMSE_s$ calculated using experimental data ($1.22 \pm 0.47^\circ\text{C}$), leading to an
329 overestimation of the NN performances (up to 150%). This observation could be explained by
330 the fact that the NN are trained using noiseless synthetic data. Indeed, the noise of the measured
331 data is mainly due to the uncertainty of the thermocouple ($\pm 0.2^\circ\text{C}$). To limit the
332 underestimation of the RMSE of NN trained with synthetic data and tested on synthetic data,
333 different noise levels were added to the synthetic test data. However, in all tested cases, the
334 $RMSE_s$ were underestimated in comparison to the RMSEs calculated on experimental data
335 (Figure 9).

336

337 **3.4. Impact of additional synthetic data**

338 Previously, NN models were trained with experimental and synthetic datasets generated from
339 10 cold chain scenarios. Now a question is: what is the impact of the choice of the scenarios?
340 Can the model train on synthetic data be improved by adding some random scenarios?

341 In order to answer this question, 50 additional random scenarios were generated and used as
342 input to the thermal model to generate synthetic data. It should be reminded that realistic
343 scenarios require field studies.

344

345 **3.4.1 Impact of scenarios used for training**

346 The performance of NN trained with the synthetic data described in section 2.3.2 are compared
347 with the performances of NN trained with synthetic data of scenarios generated randomly with
348 the thermal model by varying the time-temperature evolution of inlet air temperature. The
349 results are presented in the Figure 10 and showed that NNs trained on synthetic data generated
350 from random scenarios performed similarly to NNs trained on realistic scenarios. This
351 observation is of interest as it implies that NN can be trained without accurate information of
352 the given cold chain. Thus, to implement product temperature prediction using wireless
353 temperature sensor and NN, it is not necessary to conduct a complete field study to identify
354 representative scenario.

355

356 **3.4.2 Impact of increasing the dataset's size**

357 Once a thermal model is developed, it is easy to generate large synthetic datasets from numerous
358 synthetic cold chain scenarios. This represents the main advantage of synthetic data in
359 comparison to the generation of experimental data. With a large dataset, it is expected that the
360 NN performance would improve significantly, allowing one to achieve the performance of an
361 NN trained on experimental data. In Figure 11, the impact of the number of random scenarios
362 added to the original dataset on the $RMSE_i$ is presented, compared to $RMSE_i$ obtained from NN
363 trained on experimental data. Overall, the average $RMSE_i$ is similar for all tested cases (from 0

364 to 50 scenarios added to the original dataset). Adding more synthetic scenarios will not suffice
365 to overcome the drawbacks of synthetic data. However, the variance of the $RMSE_i$ decreases
366 as the number of added scenarios to the training increases. Hence, while the number of scenarios
367 does not impact the overall performance of the $RMSE_i$, it helps reducing the impact of the
368 weights' initialization, thus reducing the variance of the final model. Precautions need to be
369 taken on the development of NN when little data is used for trained as the NN is sensitive to
370 the weights' initialization. In this case, additional scenarios could help reducing the model
371 variance, thus, reducing false or non-undetected cold chain breaks.

372

373 **3.5. General discussion.**

374 The main issue to develop machine learning models to predict product temperature is to collect
375 the training data. This data may come from several sources: field measurement, experiments
376 in laboratory, or synthetic from more or less complex thermal models (Loisel et al. 2021). In
377 this study, the impact of experimental and synthetic data on the performance of machine
378 learning model was conducted. While NNs trained with experimental data showed better
379 performances, this kind of data require material investment. To be able to predict product
380 temperatures under various conditions (air velocity, product and pallet geometries...), the use
381 of physical based thermal model to generate synthetic data is promising. NNs trained on
382 experimental data performed better ($RMSE$ 10% lower in average) than NNs trained on
383 synthetic data. In addition, even though one can use only synthetic data of various
384 configurations to train NNs, the main issue concerns the method of evaluating the NN
385 performance. As seen in section 3.3. the use of synthetic data as test data leads to an
386 overestimation of the model performances. Furthermore, noise addition during testing is not
387 enough to overcome this issue. Measurement data (issued from laboratory experiments or

388 ideally from field data) should be used as test data to evaluate properly performances of NNs
389 trained with synthetic data. In other words, synthetic data can be used to train NNs but
390 experimental measurements should be used as test data. It should be noted that the results and
391 conclusions of this study are not generalizable to other applications or models with different
392 uncertainties. Results obtained with models with lower uncertainty (e.g. models taking into
393 account more detailed hydrodynamics effects) might be different from this study. There is a
394 need for further study of the effect of uncertainty on NN performances. In the view of the
395 development of more flexible predictive tool able to describe the high variability of
396 configurations encountered in the cold chain, without a tremendous work on model
397 development or experimental data generation, transfer learning methodology might be of
398 interest. The increasing availability of powerful machine learning methods that are efficient in
399 the large and highly variable set of situations encountered in the cold chain, is accompanied by
400 a growing demand for learning data. But, given the difficulty of producing experimental data,
401 it might be worth considering the use of transfer learning where one starts with a previously
402 learned model with similar data in order to learn a model for a new task, thus reducing the need
403 for new training data.

404 It is to be emphasized that the $RMSE$ was calculated including data measured before the first
405 2h. The $RMSE$ presented throughout this paper would have been lower if our experiments were
406 conducted on 24h or 48h. For this reason, the comparison of the performances with other similar
407 studies is not possible. The $RMSE_s$ could have been calculated omitting for example the first
408 two or three hours, in order to provide the information to the NN about the initial product
409 temperature. However, this would have been difficult to justify and in addition, there was not
410 sufficient information to set an appropriate cut-off time. Further work could be conducted on
411 defining an appropriate evaluation metric.

412 In order to improve the performances of machine learning models trained with synthetic data,
413 several studies added noise to the training data. Indeed, contrary to the experimental data, the
414 synthetic data is noiseless. Adding noise to the synthetic data could describe more accurately
415 the experimental data. To evaluate the noise impact on performance, a comparison between
416 noiseless synthetic data, synthetic data with standard deviation of 0.1°C (corresponding to \pm
417 0.2°C uncertainty of the sensor used in the experimentation, 95% of Confidence Interval), 0.2°C
418 and 0.5°C was conducted. However, no difference was found in terms of performances (results
419 not shown). Further work needs to be conducted in order to improve models trained with
420 synthetic data.

421 There are many types of NNs. In this study, Mulit-Layer Perceptrons were used. This choice
422 was made since our configuration was simple (one level of a pallet) and our preliminary tests
423 showed good results using them. The comparison of different types of NN was out of the scope
424 of this study. In further studies, focusing on more complex configurations (pallet, equipment,
425 ...), other types of NNs could be used such as RNN that are better adapted to temporal data
426 (Jaeger 2002), Convolutional Neural Networks (CNN) that are better adapted to spatial data (Le
427 Cun et al. 1990), or other methods combining both (Convolutional Recurrent Neural Networks
428 - CRNN) (Zuo et al. 2015).

429 Finally, such models to predict in real time the temperature could be associated with anomaly
430 detection algorithms in order to alert operators when cold chain breaks occur or are about to
431 occur. This would allow operators to prevent cold chain breaks by implementing corrective
432 measures to reduce the food quality degradation, ensure food safety and reducing waste
433 (Achenchabe et al. 2021).

434

435 **4. Conclusion and perspectives**

436 An experimental set-up and a physical-based model were developed to generate two datasets of
437 air and product temperatures in a pallet of apples. The objective of this study was to compare
438 performances of neural networks trained with the experimental and synthetic dataset. The main
439 conclusions are as follows:

- 440 a) Neural networks trained with experimental dataset showed better performances (20 to
441 40%) in comparison to the one trained with synthetic dataset.
- 442 b) Sensor position inside the pallet is a determining factor to predict the product
443 temperatures by neural networks.
- 444 c) Similar results were obtained from models trained with synthetic data generated from
445 realistic scenarios and from random scenarios.
- 446 d) Increasing the synthetic training dataset with 10 to 50 additional scenarios did not
447 significantly improve the model precision but reduced the model variance.
- 448 e) Models' precision is increasing over measurement time. The uncertainty of the
449 prediction during the first hours should be considered.

450

451 The implementation of such methodology in the cold chain permits to envision the preservation
452 of food quality and safety and to reduce waste. The use of neural networks would allow, in real
453 time, the prediction of product temperatures in a cold chain using wireless sensors placed in the
454 pallets. This would help operators to detect and prevent cold chain breaks on time.

455 **Acknowledgement**

456 The research leading to this result has received funding from Région Ile de France through the
457 Réseau Francilien en Sciences Informatiques (DIM RFSI).

458

459 **References**

460

461 Achenchabe, Y., Bondu, A., Cornuéjols, A., & Dachraoui, A. (2021). Early classification of time series. *Machine*
462 *Learning* 110, 1481–1504. <https://doi.org/10.1007/s10994-021-05974-z>

463 Ambaw, A., Fadiji, T., & Opara, U. L. (2021). Thermo-Mechanical Analysis in the Fresh Fruit Cold Chain: A
464 Review on Recent Advances. *Foods*, 10(6), 1357. <https://doi.org/10.3390/foods10061357>

465 Badia-Melis, R., Qian, J.P., Fan, B.L., Hoyos-Echevarria, P., Ruiz-García, L., & Yang, X. T. (2016). Artificial
466 Neural Networks and Thermal Image for Temperature Prediction in Apples. *Food Bioprocess Technol* 9, 1089–
467 1099. <https://doi.org/10.1007/s11947-016-1700-7>

468 Bouzembrak, Y., Klüche, M., Gavai, A., & Marvin, H. J. P. (2019). Internet of Things in food safety: Literature
469 review and a bibliometric analysis. *Trends in Food Science & Technology*, 94(Complete), 54-64.
470 <https://doi.org/10.1016/j.tifs.2019.11.002>

471 Derens, E., Palagos, B., & Guilpart, J. (2006). The cold chain of chilled products under supervision in France.
472 Paper presented at the In 13th world congress of food science & technology (p. 823). Nantes, France: EDP
473 Sciences. <https://doi.org/10.1051/IUFoST:20060823>

474 Nunes, M. C., Nicometo, M., Emond, J. P., Melis, R. B., & Uysal, I. (2014). Improvement in fresh fruit and
475 vegetable logistics quality: berry logistics field studies. *Philos Trans A Math Phys Eng Sci*, 372(2017), 20130307.
476 <https://doi.org/10.1098/rsta.2013.0307>

477 Duret, S., Hoang, H. M., Flick, D., & Laguerre, O. (2014). Experimental characterization of airflow, heat and mass
478 transfer in a cold room filled with food products. *International Journal of Refrigeration*, 46, 17-25.
479 <https://doi.org/10.1016/j.ijrefrig.2014.07.008>

480 Hoang, H. M., Akerma, M., Mellouli, N., Montagner, A. L., Leducq, D., & Delahaye, A. (2021). Development of
481 deep learning artificial neural networks models to predict temperature and power demand variation for demand
482 response application in cold storage. *International Journal of Refrigeration*, 131, 857-873.
483 <https://doi.org/10.1016/j.ijrefrig.2021.07.029>

- 484 IIR. (2021). International Institute of Refrigeration, The carbon Footprint of the cold chain: 7th Informatory Note
485 on Refrigeration and Food. Paris: International Institute of Refrigeration.
486 <http://dx.doi.org/10.18462/iir.INfood07.04.2021>
- 487 Jaeger, H. (2002). Tutorial on training recurrent neural networks, covering BPPT, RTRL, EKF and the "echo state
488 network" approach (Vol. 5, No. 01, p. 2002). Bonn: GMD-Forschungszentrum Informationstechnik.
- 489 James, S. J., & James, C. (2010). The food cold-chain and climate change. *Food Research International*, 43(7),
490 1944-1956. <https://doi.org/10.1016/j.foodres.2010.02.001>
- 491 Laguerre, O., Hoang, H. M., & Flick, D. (2013). Experimental investigation and modelling in the food cold chain:
492 Thermal and quality evolution. *Trends in Food Science & Technology*, 29(2), 87-97.
493 <https://doi.org/10.1016/j.tifs.2012.08.001>
- 494 O. Laguerre, S. Duret, H.M. Hoang, & D. Flick (2014), Using simplified models of cold chain equipment to assess
495 the influence of operating conditions and equipment design on cold chain performance, *International Journal of*
496 *Refrigeration*, Volume 47, Pages 120-133. <https://doi.org/10.1016/j.ijrefrig.2014.07.023>
- 497 O. Laguerre, E. Derens, & D. Flick (2018), Modelling of fish refrigeration using flake ice, *International Journal of*
498 *Refrigeration*, Volume 85, Pages 97-108. <https://doi.org/10.1016/j.ijrefrig.2017.09.014>
- 499 O. Laguerre, A. Denis, N. Bouledjeraf, S. Duret, E. Derens, J. Moureh, C. Aubert, & D. Flick (2022), Heat transfer
500 and aroma modeling of fresh fruit and vegetable in cold chain: Case study on tomatoes, *International Journal of*
501 *Refrigeration*, Volume 133, Pages 133-144. <https://doi.org/10.1016/j.ijrefrig.2021.10.009>
- 502
- 503 Le Cun, Y., Boser, B., Denker, J., Henderson, D., Howard, R., Hubbard, W., & Jacquel, L. (1990). Handwritten
504 Digit Recognition with a Back-Propagation. *Network Advances in Neural Information Processing Systems 2*:
505 Morgan Kaufmann Publishers Inc.
- 506 Loisel, J., Duret, S., Cornuéjols, A., Cagnon, D., Tardet, M., Derens-Bertheau, E., & Laguerre, O. (2021). Cold
507 chain break detection and analysis: Can machine learning help? *Trends in Food Science & Technology*, 112, 391-
508 399. <https://doi.org/10.1016/j.tifs.2021.03.052>
- 509 Mellouli N., Akerma M., Hoang M., Leducq D., & Delahaye A. (2019). Deep Learning Models for Time Series
510 Forecasting of Indoor Temperature and Energy Consumption in a Cold Room. In: Nguyen N., Chbeir R., Exposito

- 511 E., Aniorté P., Trawiński B. (eds) Computational Collective Intelligence. ICCCI 2019. Lecture Notes in Computer
512 Science, vol 11684. Springer, Cham. https://doi.org/10.1007/978-3-030-28374-2_12
- 513 Mercier, S., & Uysal, I. (2018). Neural network models for predicting perishable food temperatures along the
514 supply chain. *Biosystems Engineering*, 171, 91-100. <https://doi.org/10.1016/j.biosystemseng.2018.04.016>
- 515 Ndraha, N., Hsiao, H.-I., Vljacic, J., Yang, M.-F., & Lin, H.-T. V. (2018). Time-temperature abuse in the food cold
516 chain: Review of issues, challenges, and recommendations. *Food Control*, 89, 12-21.
517 <https://doi.org/10.1016/j.foodcont.2018.01.027>
- 518 Pedregosa, F., Varoquaux, G., Gramfort, A., Michel, V., Thirion, B., Grisel, O., Blondel, M., Prettenhofer, P.,
519 Weiss, R., Dubourg, V., Vanderplas, J., Passos, A., Cournapeau, D., Brucher, M., Perrot, M., & Duchesnay, E.
520 (2011). Scikit-learn: Machine Learning in Python. *Journal of Machine Learning Research*, 12(85), 2825-2830.
- 521 Thibault, J., Bergeron, S., & W. Bonin, H. (1987). On finite-difference solutions of the heat equation in spherical
522 coordinates. *Numerical Heat Transfer* 12(4): 457-474. <https://doi.org/10.1080/10407788708913597>
- 523 Van der Sman (2003), Simple model for estimating heat and mass transfer in regular-shaped foods, *Journal of*
524 *Food Engineering*, Volume 60, Issue 4, Pages 383-390, ISSN 0260-8774. [https://doi.org/10.1016/S0260-](https://doi.org/10.1016/S0260-8774(03)00061-X)
525 [8774\(03\)00061-X](https://doi.org/10.1016/S0260-8774(03)00061-X)
- 526 Xiao, X., He, Q., Fu, Z., Xu, M., & Zhang, X. (2016). Applying CS and WSN methods for improving efficiency
527 of frozen and chilled aquatic products monitoring system in cold chain logistics. *Food Control*, 60, 656-666.
528 <https://doi.org/10.1016/j.foodcont.2015.09.012>
- 529 Zuo, Z., Shuai, B., Wang, G., Liu, X., Wang, X., Wang, B., & Chen, Y. (2015). Convolutional recurrent neural
530 networks: Learning spatial dependencies for image representation. Paper presented at the 2015 IEEE Conference
531 on Computer Vision and Pattern Recognition Workshops (CVPRW), June 7th-12th 2015.

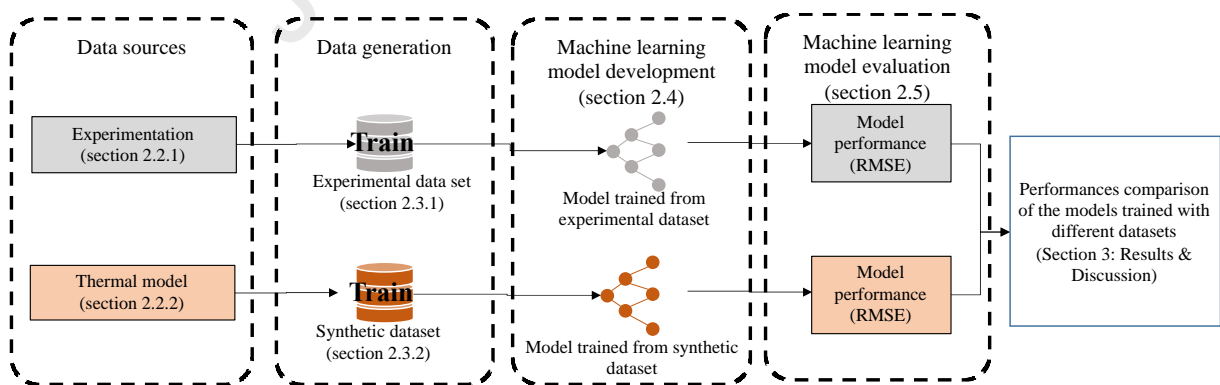
532

533

534

535

536
537
538
539
540
541
542
543
544
545
546
547
548



549

550 **Figure 1: Overview of the methodology processed to compare performances of machine**
551 **learning models trained with two types of datasets.**

552

553

554

555

556

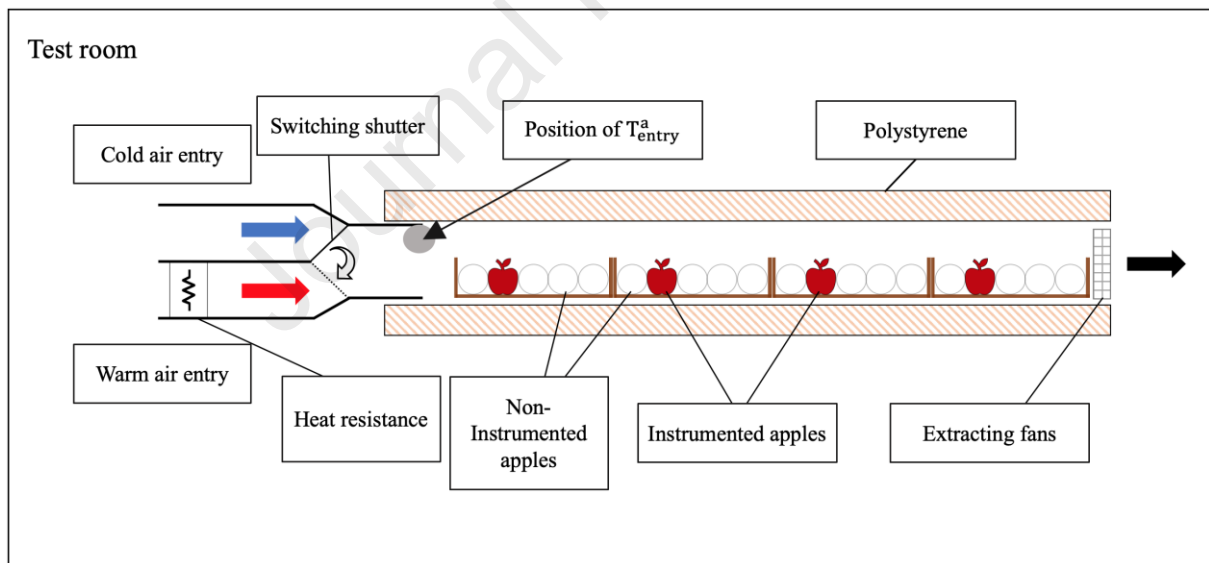
557

558

559

560

561

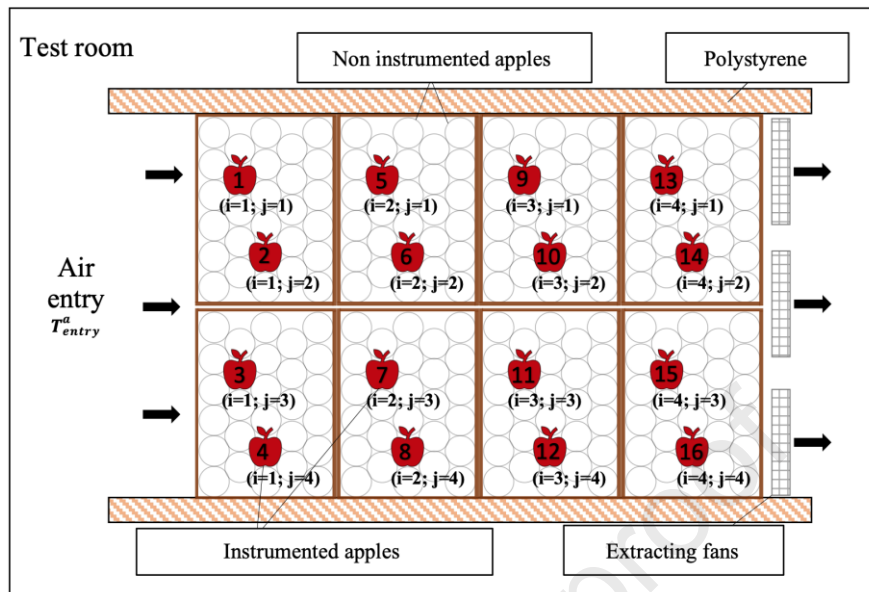


562

563

(a) Side view

564



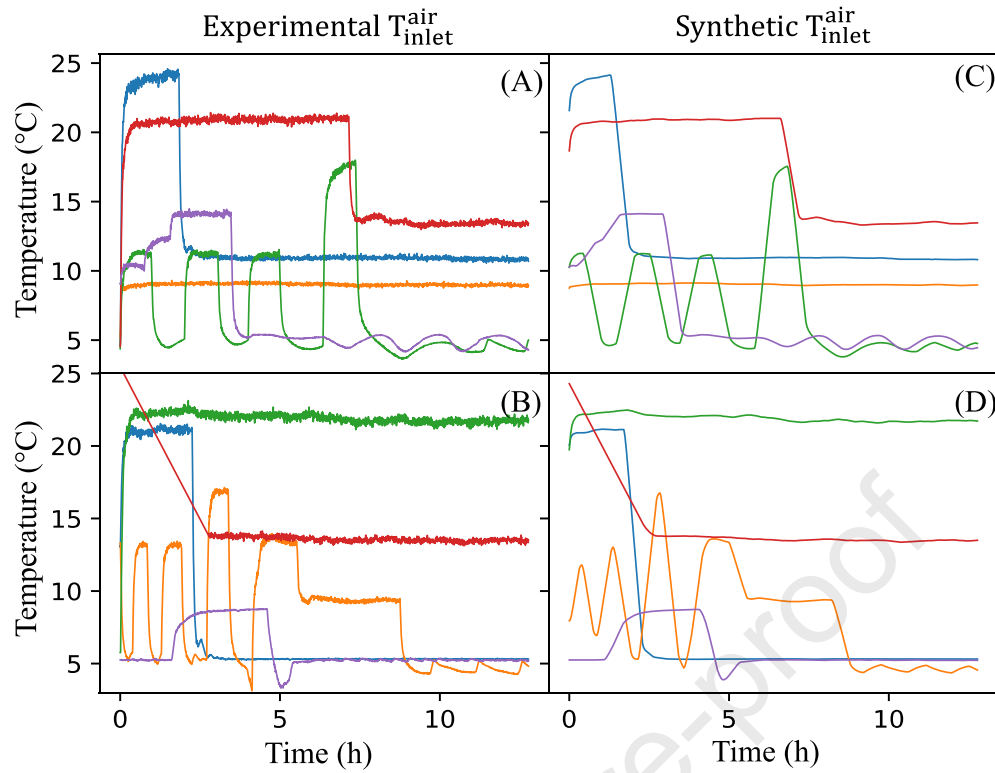
565

566

(b) Top view

567 **Figure 2: Experimental set up. (a) Side view (sidewall open to show product arrangement**
 568 **inside) (b) Top view. Red apples represent the instrumented product, the value over them**
 569 **corresponds to the zone number. White circles are non-instrumented apples.**

570

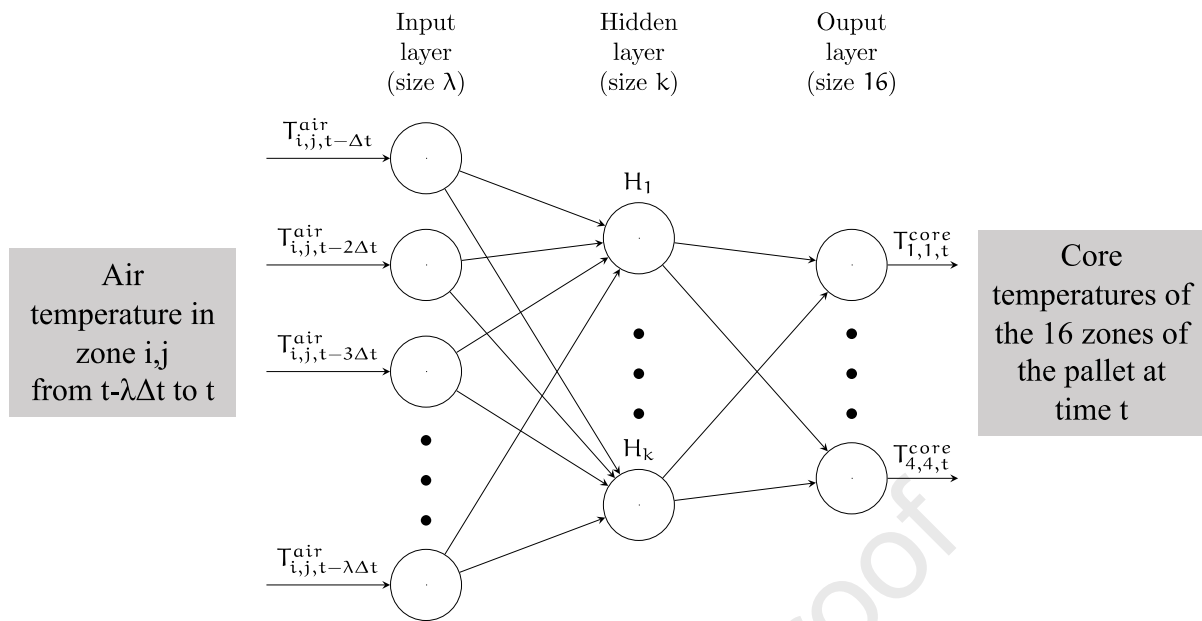


571

572 **Figure 3: Inlet air temperature profiles of the studied cold chain scenarios: (A) and (B) -**573 **Experimental profiles, (C) and (D) - Synthetic profiles (experimental profiles were**574 **smoothed to obtain profiles of the thermal model input). Five profiles are plotted in each**575 **graph for readability purpose.**

576

577

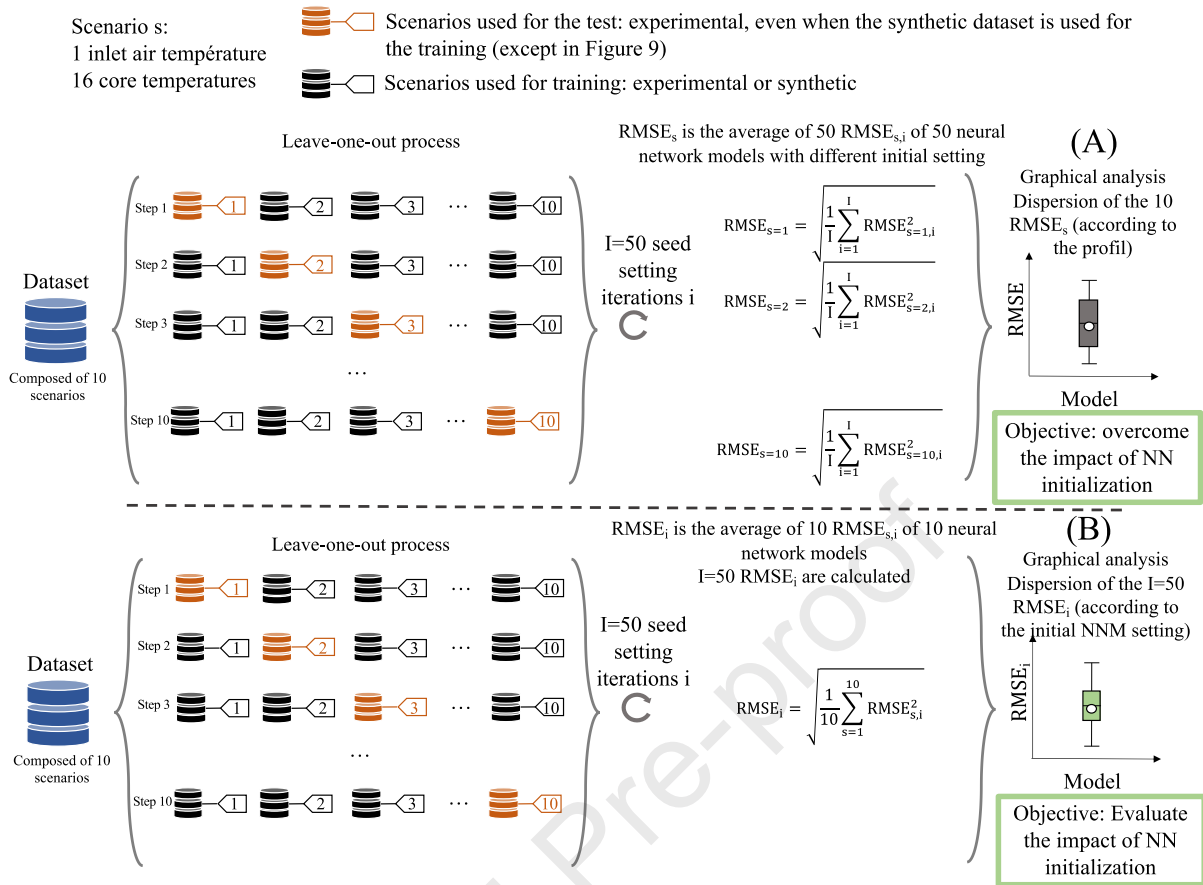


578

579 **Figure 4 : Schematic representation of a 1- hidden layer NN of size k with air temperature**
 580 **at one position from time $t-\lambda\Delta t$ to time t in the input layer and 16 product core**
 581 **temperatures at time t in the output layer.**

582

583

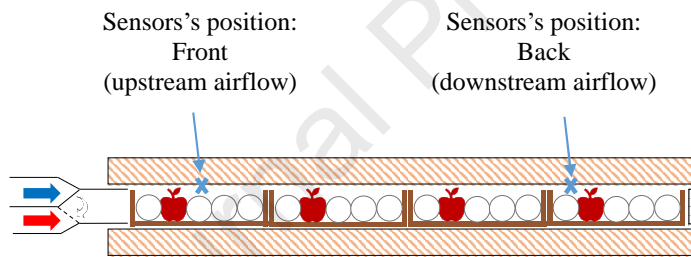
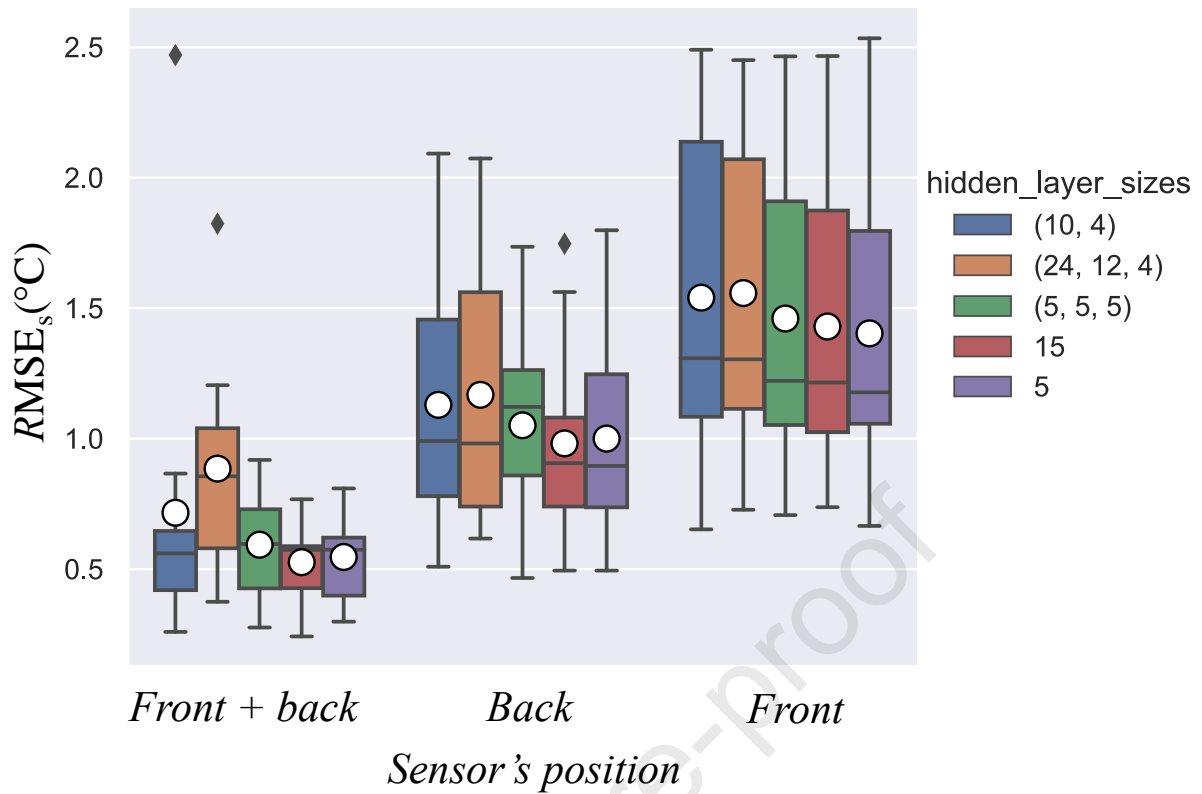


584

585 **Figure 5: Method used to train (LOO process) and evaluate (RMSE) NN: (A) Method to**
 586 **evaluate the model's performance according to various parameters (sensor, training data**
 587 **type) (B) Method to evaluate the impact of the NN initialization on the NN performance**

588

589



590

591

592 **Figure 6 : Impact of sensor's position on the distribution of the $RMSE_s$ for five NN**593 **models trained with experimental data. Boxplots represents the distribution of the 10**594 **$RMSE_s$ resulting from the leave-one-out cross validation. White dots and black**595 **diamonds represent the average of the 10 $RMSE$ and the outliers, respectively.**

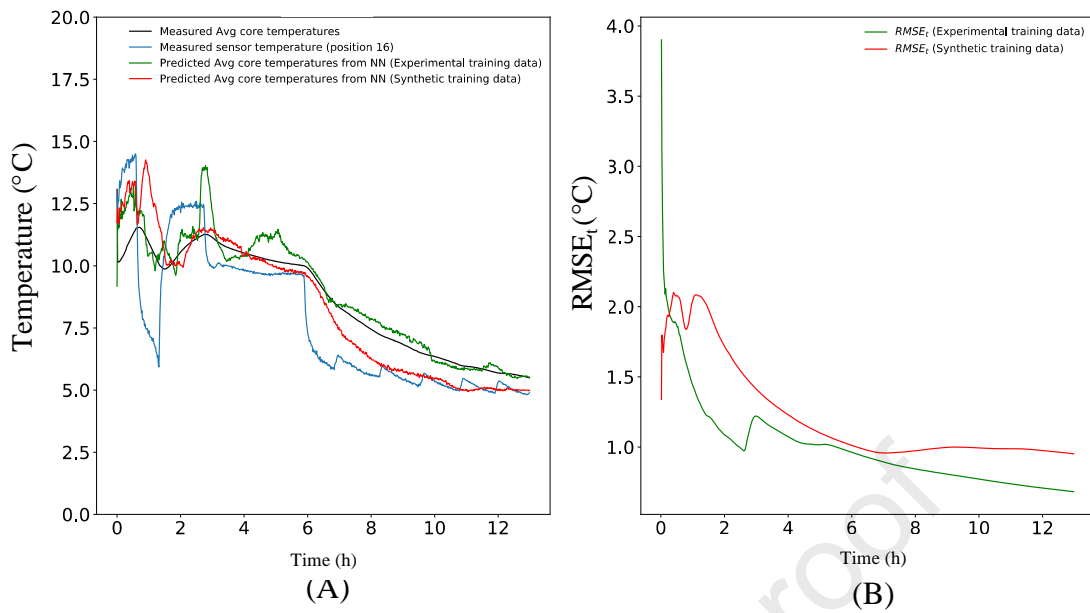
596

597

598

599

600



601

602 **Figure 7 : (A) Temperature evolution over 12h of one cold chain scenario: Blue line - sensor**
 603 **measured air temperature (input of NN); Black line - experimental core temperature; Green line**
 604 **- core temperature predicted by NN trained with experimental data; Red line - core temperature**
 605 **predicted by NN trained with synthetic data. These core temperatures are the average value of 16**
 606 **apples (B) Evolution of the $RMSE_t$ of the NN trained with experimental and synthetic data (green**
 607 **and red lines, respectively). Results obtained with the sensor at the back of the pallet with the NN**
 608 **(24,12,4).**

609

610

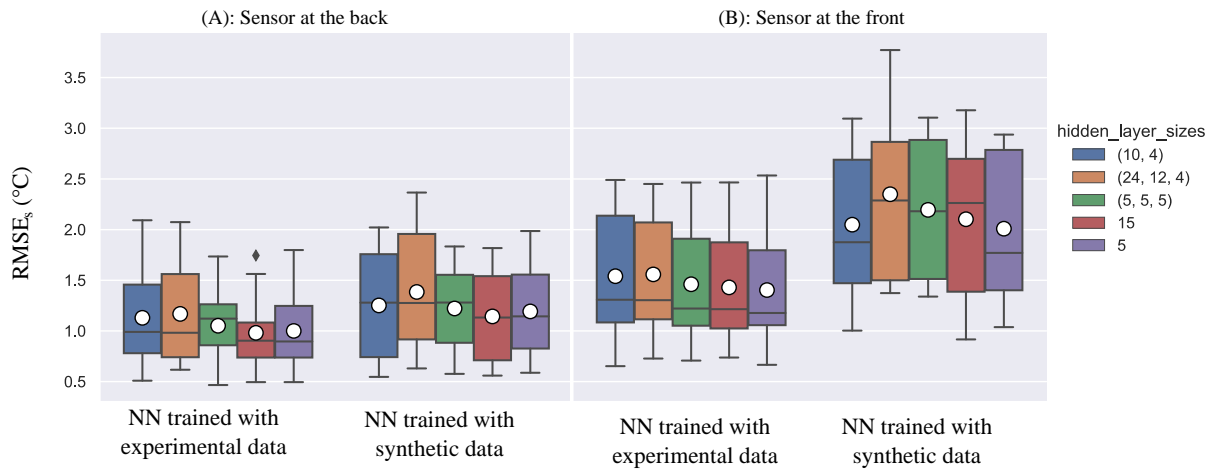
611

612

613

614

615



616

617 **Figure 8: RMSE_s distribution of five NN trained with experimental and synthetic data.**618 **(A) Sensor measuring air temperature at the back (B) Sensor measuring air temperature**619 **at the front. Boxplots represents the distribution of the 10 RMSE_s resulting from the leave-**620 **one-out cross validation (see section 2.5 for further details on RMSE_s calculation). White**621 **dots and black diamonds represent the average of the 10 RMSE and the outliers,**622 **respectively.**

623

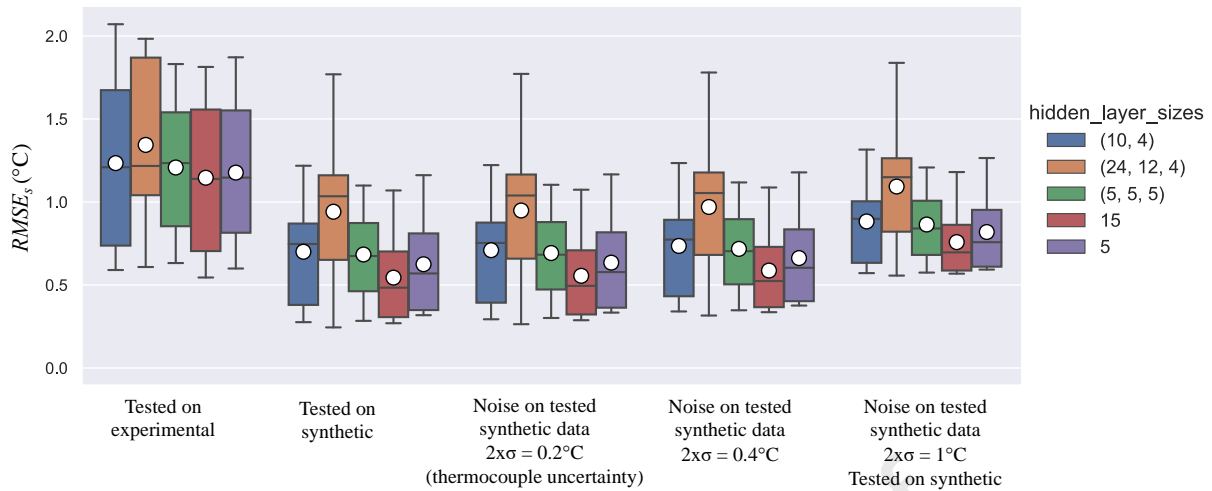
624

625

626

627

628



629

630 **Figure 9: $RMSE_s$ distribution of five NN trained with synthetic data and tested on**
 631 **experimental data, noiseless synthetic data and synthetic data with three different noise**
 632 **($2x\sigma = 0.2^{\circ}C$ to represent thermocouple uncertainty). The sensor is placed at the back of**
 633 **the pallet. Boxplots represents the distribution of the 10 $RMSE_s$ resulting from the**
 634 **leave-one-out cross validation (see section 2.5 for further details on $RMSE_s$ calculation).**

635

636

637

638

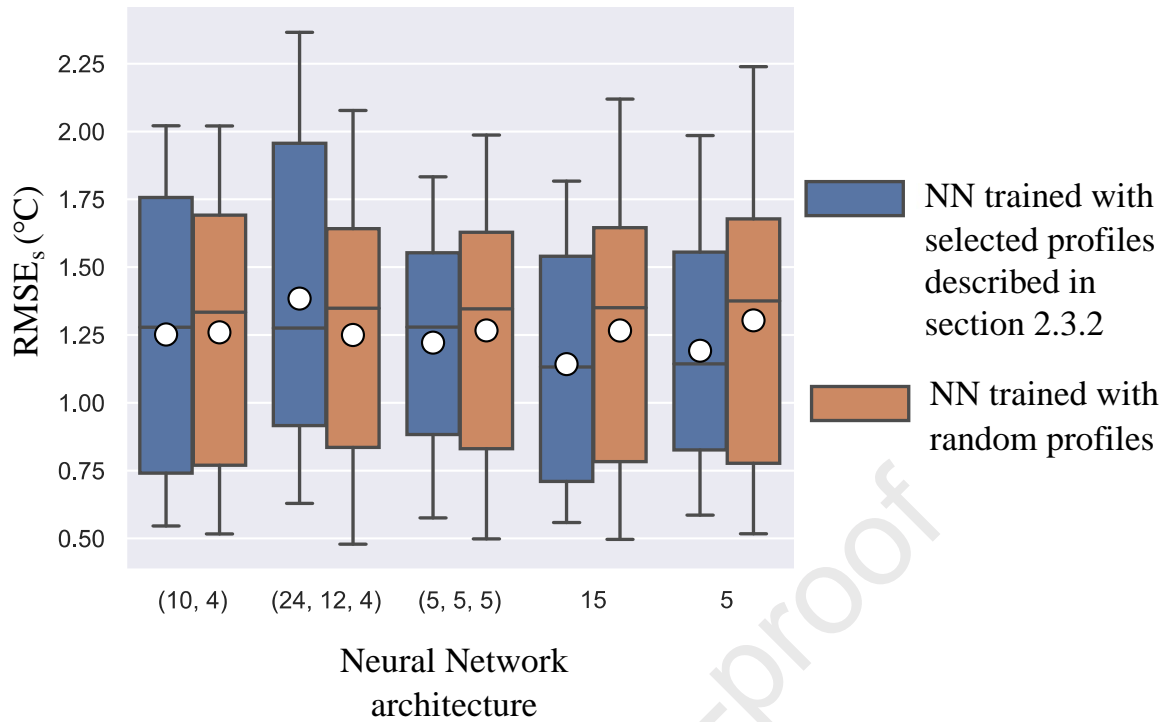
639

640

641

642

643



644

645 **Figure 10: $RMSE_s$ distribution of five NN trained by synthetic data using the 10 scenarios**
646 **described in section 2.3.2 (blue) and 10 scenarios generated randomly. Results presented with the**
647 **sensor placed at the back of the pallet.**

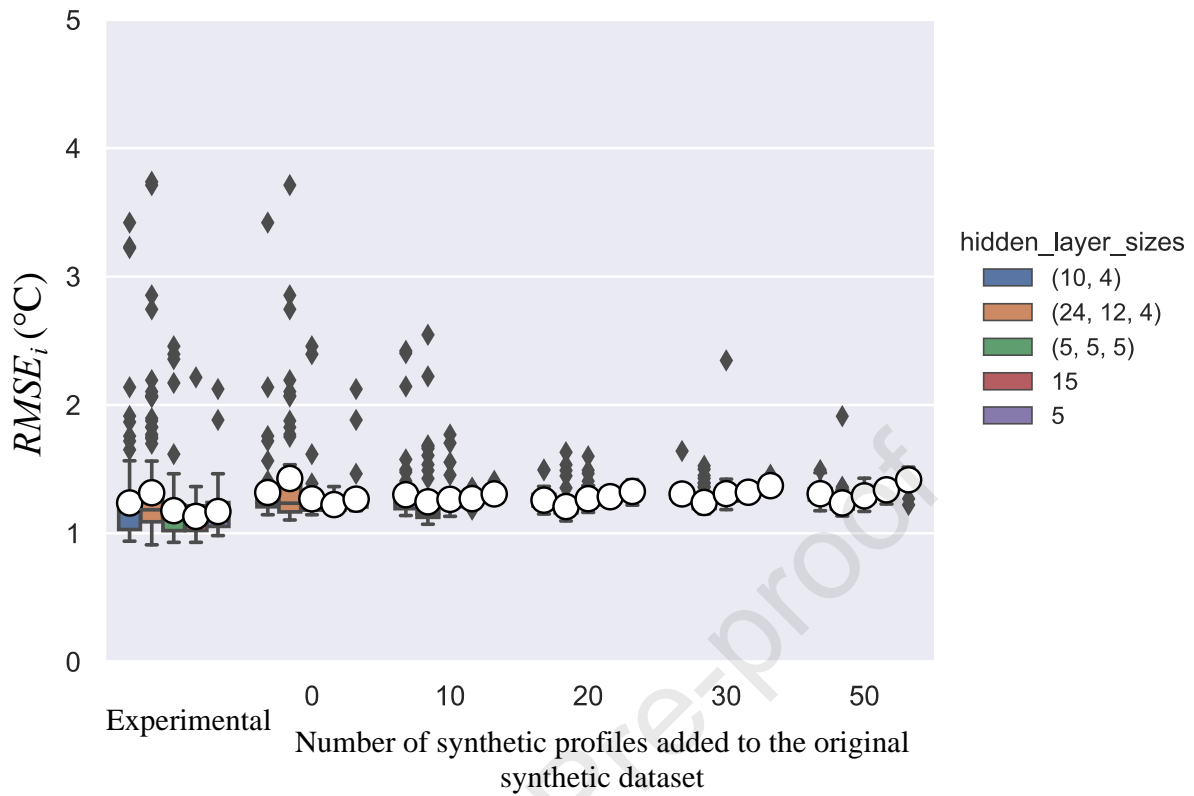
648

649

650

651

652



Training Dataset

653

654 **Figure 11: Impact of the number of scenarios added to the original dataset on the $RMSE_i$**
 655 **(criteria dependent of NN initialization – see section 2.5)**

656

657

658

659

660

661

662

Highlight

- Product temperature in a pallet is predicted with neural networks trained on experimental and synthetic data
- Neural networks trained using experimental data give better performance
- Increasing the size of the synthetic dataset helps reducing the model's variance
- Noise addition to the synthetic dataset did not improve the model's performance
- Realistic time temperature scenarios based from field studies are not required to train machine learning model

Conflict of Interest and Authorship Conformation Form

Please check the following as appropriate:

- All authors have participated in (a) conception and design, or analysis and interpretation of the data; (b) drafting the article or revising it critically for important intellectual content; and (c) approval of the final version.
- This manuscript has not been submitted to, nor is under review at, another journal or other publishing venue.
- The authors have no affiliation with any organization with a direct or indirect financial interest in the subject matter discussed in the manuscript
- The following authors have affiliations with organizations with direct or indirect financial interest in the subject matter discussed in the manuscript:

Author's name	Affiliation
Julie Loisel	Université Paris-Saclay, UMR MIA-Paris, AgroParisTech, INRAE, 75005 Paris, France Université Paris-Saclay, FRISE, INRAE, 92761 Antony, France
Antoine Cornuéjols	Université Paris-Saclay, UMR MIA-Paris, AgroParisTech, INRAE, 75005 Paris, France
Onrawee Laguerre	Université Paris-Saclay, FRISE, INRAE, 92761 Antony, France
Margot Tardet	BIOTRAQ, 6 Rue Montalivet, 75008 Paris, France
Dominique Cagnon	BIOTRAQ, 6 Rue Montalivet, 75008 Paris, France
Olivier Duchesne de Lamotte	BIOTRAQ, 6 Rue Montalivet, 75008 Paris, France
Steven Duret	Université Paris-Saclay, FRISE, INRAE, 92761 Antony, France